

Responses to Referee #1's comments

We are grateful to the reviewers for their valuable and helpful comments on our manuscript “**Molecular-level study on the role of methanesulfonic acid in iodine oxoacids nucleation**” (MS No.: egusphere-2023-2084). We have revised the manuscript carefully according to reviewers' comments. The point-to-point responses to the Referee #1's comments are summarized below:

Referee comments:

Li et al. explored the role of methanesulfonic acid (MSA) in iodine oxoacids nucleation. Detailed molecular-level mechanisms of cluster formation were studied using quantum chemical methods and cluster dynamics, providing theoretical evidence for the contribution of MSA to the formation of marine iodine clusters. After carefully reading the manuscript, I find that the main argument that MSA may enhance the nucleation rate of iodine oxoacids is convincing. The contribution of MSA to the formation of marine iodine particles remains an open question because other acids and bases such as sulfuric acid and amines may also affect the HIO₃-HIO₂ nucleation process in the real atmosphere - as the authors have addressed at the end of this manuscript - while this study provides an important theoretical basis for this question. This manuscript is well written. I recommend it be accepted by *Atmospheric Chemistry and Physics*. A few minor comments on the interpretation of the theoretical results are given below.

Response: Thanks sincerely for the reviewer's professional and positive comments. We have revised the manuscript accordingly. The detailed point-to-point responses are listed as follows.

General comments:

Comment 1: Figures 1-3 seem to suggest that the significant enhancement of MSA on HIO₃-HIO₂ nucleation is robust against the uncertainties of cluster stability. However, would it be possible to have a supplementary or appendix figure for the general audience, showing the uncertainty range of the enhancement or relative contribution of MSA to the cluster formation rate?

Response: Thanks for the reviewer's professional and helpful comments. The uncertainties of enhancement of MSA on cluster formation may stem from ACDC simulations and quantum

chemical (QC) calculations, thereby we examined how variable ACDC settings, such as condensation sink coefficient (CS), sticking factor (SF, corresponding to a sticking probability for cluster/monomer collision) and the change of calculated Gibbs free energy of cluster formation (ΔG , from quantum chemical calculations) impact the enhancement of MSA (R_{MSA}) on cluster formation rate (J). Here, the CS values ranged from $1.0 \times 10^{-4} \text{ s}^{-1}$ to $1.0 \times 10^{-2} \text{ s}^{-1}$, covering possible CS in relatively clean and polluted regions^[1,2]. The range of SF was set from 0.1 to 1.0 since sticking probabilities for neutral-neutral collisions between 0.1 and 1.0^[3].

As shown in the Figs. S15 (a) and (b), although both CS and SF affect R_{MSA} to some extent, the uncertainty range are relatively limited (CS < 32.5% and SF < 17.1%) and the results does not affect the trend and main conclusions.

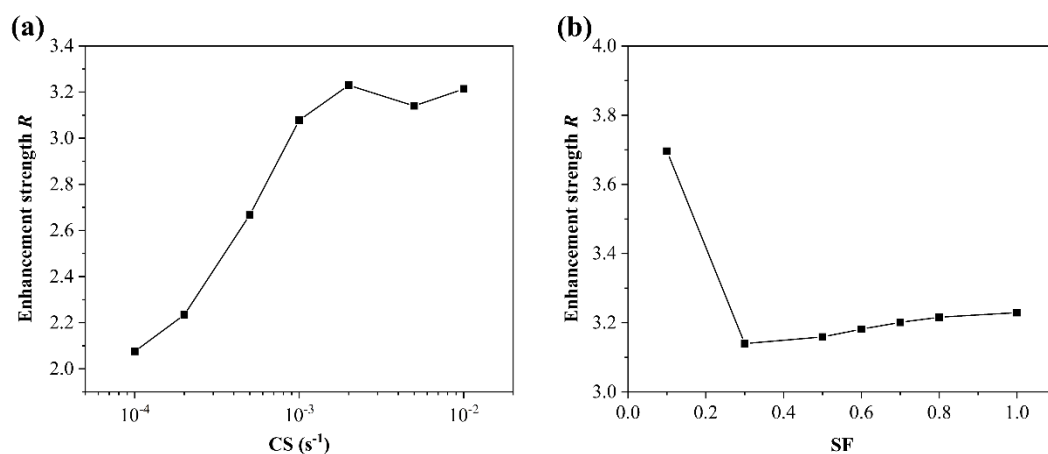


Figure S15. Variation of enhancement strength R of MSA with (a) condensation sink coefficient (CS) and (b) sticking factor (SF) for $\text{HIO}_3\text{-HIO}_2\text{-MSA}$ system at $T = 278 \text{ K}$, $[\text{HIO}_3] = 1.0 \times 10^7$, $[\text{HIO}_2] = 2.0 \times 10^5$, and $[\text{MSA}] = 1.0 \times 10^7 \text{ molec. cm}^{-3}$.

In addition, the potential uncertainty of quantum chemical calculations is ultimately manifested in the calculated ΔG values. As reported by Kupiainen^[4] et al. (2012), the differences between the computational (DFT//RI-CC2 method) and experimental ΔG values are about 1 kcal mol^{-1} or less^[5]. Accordingly, Almedia^[3] et al. (2013) calculated the uncertainty range of ACDC simulated cluster formation resulting from QC calculations by adjusting the binding energy ($\pm 1 \text{ kcal mol}^{-1}$). Further given the consistency of our research framework (DFT//RI-CC2 + ACDC) with Almedia et al. (2013), herein we have performed the uncertainty analysis of R_{MSA} caused by QC calculations through adding or subtracting 1 kcal mol^{-1} from the ΔG (using $\Delta G_{278\text{K}}$ as a reference). The figure below presents the uncertainty analysis results of

J and R_{MSA} at $T = 278$ K, $\text{CS} = 2.0 \times 10^{-3} \text{ s}^{-1}$, $[\text{HIO}_3] = 10^7$, $[\text{HIO}_2] = 2.0 \times 10^5$, $[\text{MSA}] = 10^6 - 10^8 \text{ molec. cm}^{-3}$.

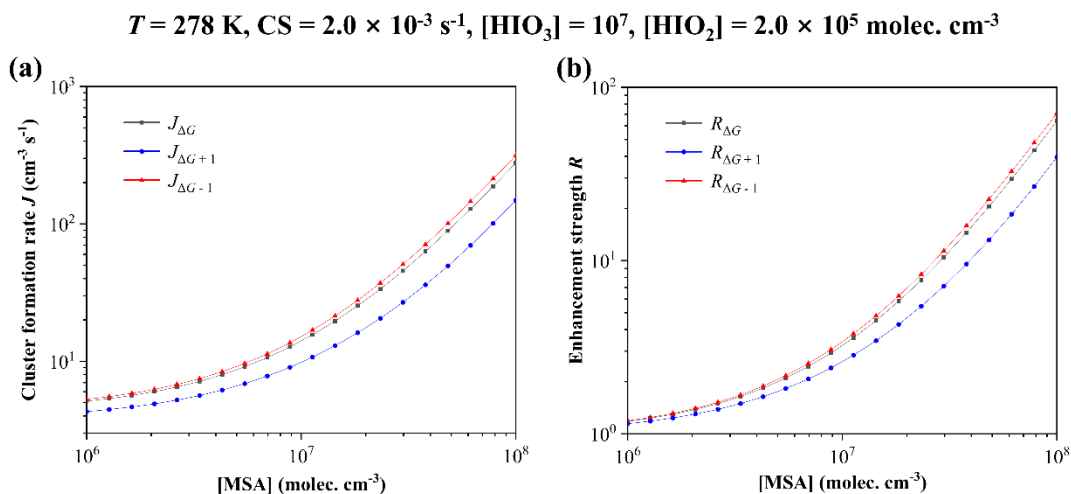


Figure S16. Cluster formation rate J (a) and enhancement strength R of MSA (b) as a function of $[\text{MSA}] = 10^6 - 10^8 \text{ molec. cm}^{-3}$, with different energy of $\Delta G_{278\text{K}}$ (black line), $\Delta G_{278\text{K}} + 1$ (blue line), $\Delta G_{278\text{K}} - 1$ (red line), at $T = 278$ K, $\text{CS} = 2.0 \times 10^{-3} \text{ s}^{-1}$, $[\text{HIO}_3] = 10^7$, $[\text{HIO}_2] = 2.0 \times 10^5 \text{ molec. cm}^{-3}$.

Here, we have added the results of R_{MSA} under different CS, SF and ΔG to the revised supporting file, and for the convenience of the review, we have copied Figures S15-S16 and the corresponding analysis as following: “Here, the potential uncertainties may stem from ACDC simulations and quantum chemical (QC) calculations, we examined the effect of condensation sink coefficient (CS), sticking factor (SF) and calculated ΔG of clusters on enhancement of MSA to the cluster formation rate. The CS values ranged from $1.0 \times 10^{-4} \text{ s}^{-1}$ to $1.0 \times 10^{-2} \text{ s}^{-1}$, covering possible CS in relatively clean and polluted regions^[1, 2]. The range of SF was set from 0.1 to 1.0 since sticking probabilities for neutral-neutral collisions between 0.1 and 1.0^[3]. Both the CS and SF slightly affect the enhancement of MSA, with limited uncertainty range of $\text{CS} < 32.5\%$ and $\text{SF} < 17.1\%$ (Fig. S15). As reported by Kupiainen^[4] et al. (2012), the differences between the computational (DFT//RI-CC2 method) and experimental ΔG values are about 1 kcal mol^{-1} or less^[5]. Accordingly, Almedia^[3] et al. (2013) calculated the uncertainty range of ACDC simulated cluster formation resulting from QC calculations by adjusting the binding energy ($\pm 1 \text{ kcal mol}^{-1}$). Further given the consistency of our research framework (DFT//RI-CC2 + ACDC) with Almedia et al. (2013), herein we have performed the uncertainty

analysis of R_{MSA} caused by QC calculations through adding or subtracting 1 kcal mol⁻¹ from the ΔG (using $\Delta G_{278\text{K}}$ as a reference). As shown in Table S8 and Fig. S16, adjusting the $\Delta G_{278\text{K}}$ of clusters by ± 1 kcal mol⁻¹ resulted in a minor variation in J and R of MSA, with the overall trend remaining consistent.”

Comment 2: I found it challenging to interpret the relative importance of the MSA-involved path in HIO₃-HIO₂-MSA nucleation. Figure 3a shows that the MSA-involved path is a major path (74 %), yet this was simulated with a [MSA] 5 times of [HIO₃]. With the same [MSA] and [HIO₃], the MSA-involved path was expected to contribute ~20 %, showing that MSA was a bit less efficient than HIO₃ in clustering with HIO₂. This comparatively lower efficiency does not affect the main conclusion as the [MSA] may exceed [HIO₃] in atmospheric environments. However, Figures 4 and 5 show a high enhancement factor (> 2) with the same [MSA] and [HIO₃]. This high enhancement factor indicates that MSA is more efficient than what I interpreted above. I hope this can be clarified in the revised manuscript.

Response: This is a very insightful point – thanks for bringing it up. Indeed, as expertly assessed by the reviewer, HIO₃ undergo clustering with HIO₂ more efficiently than MSA due to the lower contribution of MSA-involved pathway (~20%) at same concentrations of HIO₃ and MSA (10⁷ molec. cm⁻³). However, in this case, the involvement of MSA in nucleation shows a high enhancement factor (> 2) for rate J , which is indeed the point that may confuse the reader. Accordingly, we explored the underlying nucleation mechanism under the focused condition: $T = 278\text{K}$, $CS = 2.0 \times 10^{-3} \text{ s}^{-1}$, (a) $[\text{HIO}_3] = [\text{MSA}] = 1.0 \times 10^7$, and $[\text{HIO}_2] = 2.0 \times 10^5$ molec. cm⁻³. (b) $[\text{HIO}_3] = [\text{MSA}] = 1.0 \times 10^6$, and $[\text{HIO}_2] = 2.0 \times 10^4$ molec. cm⁻³.

As shown in Fig. S7, the contribution of MSA to clustering consists not only of directly forming HIO₃-HIO₂-MSA clusters (~20%), but also its ‘catalysis’ role in facilitating formation of initial HIO₃-HIO₂ clusters, e.g., (HIO₃)₁(HIO₂)₁₋₂, through a process of first participation in forming the (HIO₃)₁(HIO₂)₁₋₂(MSA)₁ clusters, and then evaporation out. Taken together, MSA promotes both HIO₃-HIO₂-MSA and HIO₃-HIO₂ clustering pathways, and its dual contribution results in a high enhancement factor (> 2).

Furthermore, to make the readers clear, we accordingly provide an explanatory account of this phenomenon as follows (Lines 227-231 in the revised manuscript): “However, the

atmospheric $[\text{HIO}_3]$ ranges widely from 10^6 to 10^8 molec. cm^{-3} . When $[\text{HIO}_3]$ is comparable or higher than $[\text{MSA}]$, the HIO_3 - HIO_2 pathway contributes more, and the R of MSA decreases with the rising $[\text{HIO}_3]$. It is worth noting that when $[\text{HIO}_3]$ is comparable to $[\text{MSA}]$, the R of MSA is greater than 2, as the contribution of MSA to clustering includes not only the direct formation of HIO_3 - HIO_2 -MSA clusters ($\sim 20\%$), but also its ‘catalysis’ role in facilitating formation of initial HIO_3 - HIO_2 clusters (Fig. S7).”

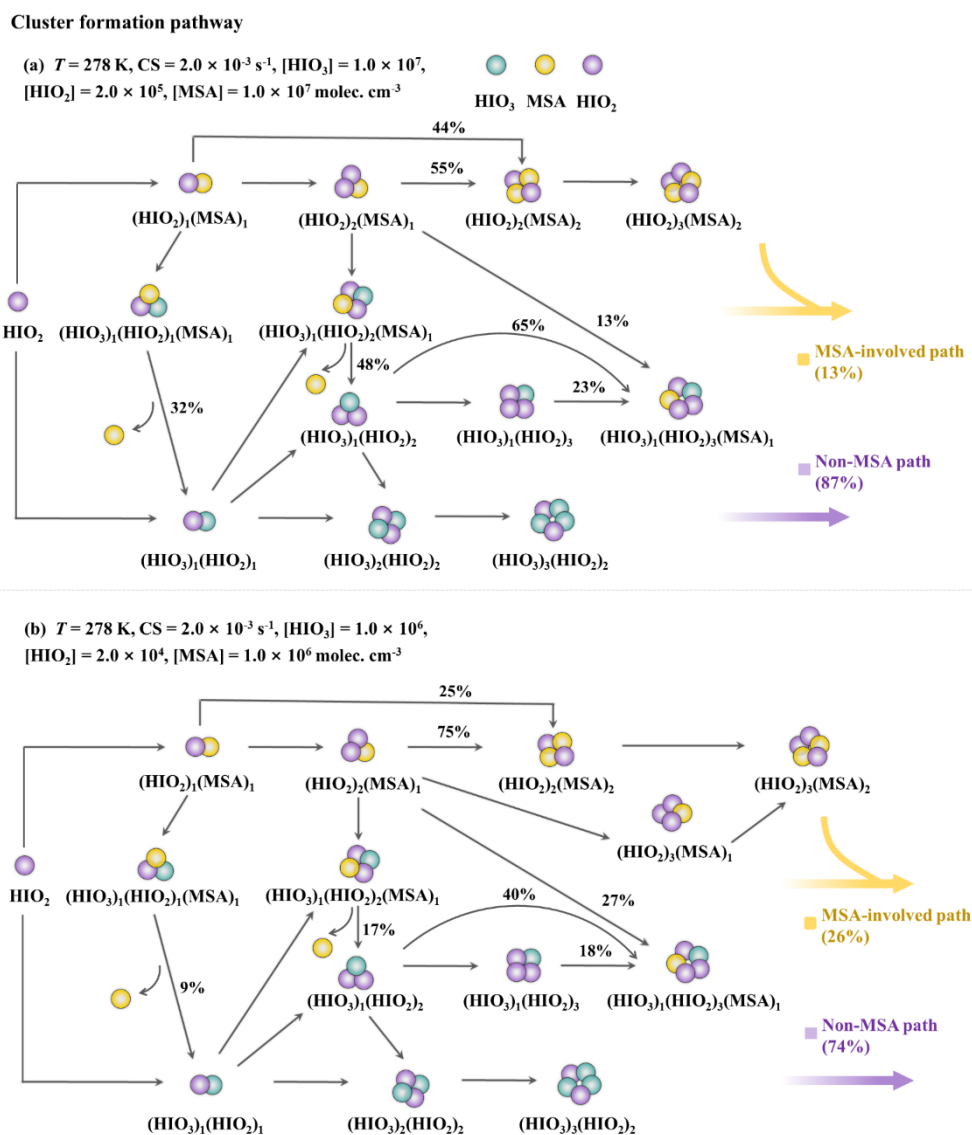


Figure S7. Main cluster growth pathway of the HIO_3 - HIO_2 -MSA nucleating system at $T = 278\text{K}$, $\text{CS} = 2.0 \times 10^{-3} \text{ s}^{-1}$, (a) $[\text{HIO}_3] = 1.0 \times 10^7$, $[\text{HIO}_2] = 2.0 \times 10^5$, and $[\text{MSA}] = 1.0 \times 10^7$ molec. cm^{-3} , (b) $[\text{HIO}_3] = 1.0 \times 10^6$, $[\text{HIO}_2] = 2.0 \times 10^4$, and $[\text{MSA}] = 1.0 \times 10^6$ molec. cm^{-3} .

Specific comments:

Comment 3: Line 180, "Overall, the results suggest that MSA's contribution to cluster formation is positively related to [MSA] but negatively linked to [HIO₃]." This sentence is correct in terms of the relative contribution but awkward. How about removing this sentence and adding discussions on the relative importance of the MSA path (see comment 2)?

Response: According to the reviewer's helpful suggestion, we have removed the mentioned sentence "Overall, the results suggest that MSA's contribution to cluster formation is positively related to [MSA] but negatively linked to [HIO₃]" in Line 180, and added the discussion of comment 2 in the revised manuscript (Lines 227-231, page 10).

Comment 4: Line 207, "To sum up, MSA can promote nucleation, particularly in marine regions characterized by lower T, lower [HIO₃] and [HIO₂]." I was confused that MSA can promote nucleation at low [HIO₂] within the context of this manuscript, as [HIO₂] is the starting point of cluster formation. This might be caused by overemphasizing the relative contribution. Also, [HIO₂] is usually associated with [HIO₃]. Replacing [HIO₃] (implicitly indicated to be independent of [HIO₂]) with [HIO₃]/[HIO₂] in some discussions may help with understanding.

Response: Certainly, as predicted by the reviewer, [HIO₂] is the starting point of cluster formation. When [HIO₂] declines, both MSA-involved and non-MSA pathway proportions decrease (see Fig. (3) in the main text). However, in this study, we draw the following conclusions based on the calculated enhancement strength (R) of MSA on nucleation, i.e., $R = J(\text{HIO}_3\text{-HIO}_2\text{-MSA}) / J(\text{HIO}_3\text{-HIO}_2)$. As [HIO₂] declines, both the numerator and denominator of R decrease. However, the numerator diminishes relatively slowly due to the introduction of MSA, enhancing the rate and retarding its decay, which results in an increased R value. Yet, in environments with higher [HIO₂], the enhancing effect of MSA will be weaker because the more efficient HIO₃ will fully combine with HIO₂, thereby resulting in a lower R .

Accordingly, following the professional advice of the reviewer, to make it clear to the readers, we add the explanation prior to the introduction of the ACDC simulations as follows: "...where [HIO₃]/[HIO₂] is a constant" in Line 150 of page 6.

Comment 5: Line 222, "observed J of $2.1 \times 10^{-4} \text{ cm}^{-3} \text{ s}^{-1}$ ". This J value is too low from a

measurement point of view. In a scatter plot showing the correlation between J and precursor concentrations, some small values of J are often given, though they might be obtained during weak or non-NPF periods. I checked the SI of Beck et al. and found that they have clarified that "Data with J -values $<$ a few $10^{-3} \text{ cm}^{-3} \text{ s}^{-1}$ are highly unreliable and reflect mainly the noise levels...". Figure 2a in their main manuscript shows that the J value is $\sim 0.1 \text{ cm}^{-3} \text{ s}^{-1}$ during typical NPF events.

Response: Thanks for these professional and rigorous suggestions. Accordingly, given the unreliability of J -values ($<$ a few $10^{-3} \text{ cm}^{-3} \text{ s}^{-1}$), we have adjusted the range of the observed cluster formation rate J of Ny-Ålesund to $10^{-3} - 10^{-1} \text{ cm}^{-3} \text{ s}^{-1}$ in Fig. 6(a). And the sentence "...the $J(\text{HIO}_3\text{-HIO}_2\text{-MSA})$ can be two orders of magnitude higher than the observed J of $2.1 \times 10^{-4} \text{ cm}^{-3} \text{ s}^{-1}$ " has been changed to "...the $J(\text{HIO}_3\text{-HIO}_2\text{-MSA})$ can be one order of magnitude higher than the observed J of $10^{-3} \text{ cm}^{-3} \text{ s}^{-1}$ " in Lines 248-249 (page 11) of the revised manuscript.

Comment 6: Figure 6. It is recommended to adjust the shaded area of field observation. Now the measured J shares a similar style with the simulated J . Some readers may wonder why there is no correlation between the measured J and $[\text{HIO}_3]$.

Response: Thanks. The reviewers' suggestion is helpful in improving the clarity of the data. Accordingly, we have changed the measured J with a different style in Fig. 6 from shaded areas to dashed lines.

Comment 7: Figure 6 caption. Please explain why there is a single line for $\text{HIO}_3\text{-HIO}_2$ while $[\text{HIO}_2]$ ranges from $2\text{e}3$ to $2\text{e}4$. Is it because of a constant $[\text{HIO}_2]/[\text{HIO}_3]$ in the simulation?

Response: As the reviewer's expert insight suggests, the reason that the rate of $\text{HIO}_3\text{-HIO}_2$ cluster formation presents as a line that increases with $[\text{HIO}_3]$ is that $[\text{HIO}_3]/[\text{HIO}_2]$ is fixed to a constant value (50, according to the field measured ratio from Sipilä et al. 2016^[6]) in the simulation. To make it clearer for the readers, we have added a description of the relationship between $[\text{HIO}_3]$ and $[\text{HIO}_2]$ to the caption of Fig.6 as: " $[\text{HIO}_3]/[\text{HIO}_2]$ is a constant".

Comment 8: Figure S5. Please give the reference for field observation data herein. It is surprising to see a high formation rate of $1\text{e}4\text{-}1\text{e}6 \text{ cm}^{-3} \text{ s}^{-1}$.

Response: According to the reviewer's suggestion, the corresponding reference (O'Dowd, et al., *J. Geophys. Res.: Atmos.*, 2002)^[7] has been cited in the caption of Figure S14 (previous Figure S5) in the revised supporting information.

Comment 9: Line 248, "...thermodynamic analyses suggest that MSA-involved clustering is nearly barrierless". I do not disagree with this statement, yet it may confuse some readers, especially considering that the horizontal axes in Figs. 5-6 are [HIO₃] rather than [HIO₂]. How about emphasizing that the HIO₂ addition, as the rate-limiting step for cluster formation and growth, is nearly barrierless?

Response: Thanks for the reviewer's professional comments. The preference for [HIO₃] as the horizontal axes in Figs. 5-6 is due to the strong correlation between NPF occurrence and observations of iodic acid^[6]. Also, in CLOUD experiments, the nucleation rates show a strong dependency on HIO₃ concentration^[8]. Conversely, there are limited available field observations of HIO₂, characterized by lower reported concentrations, despite its pivotal role in stabilizing HIO₃ cluster. Therefore, the concentration of HIO₃ is employed here as horizontal axes to present the results of cluster formation rate or enhancement strength.

Furthermore, as mentioned by the reviewer, the HIO₂ addition is the rate-limiting step for cluster formation, which leads to the significant increasement of the $J(\text{HIO}_3\text{-HIO}_2\text{-MSA})$ compared to $J(\text{HIO}_3\text{-MSA})$ (Figure S12). As shown in Figure S13, thermodynamic analysis suggest that compared with HIO₃-MSA pathway, HIO₃-HIO₂-MSA path is almost barrierless (1.24 kcal mol⁻¹) at $T = 278$ K, $[\text{HIO}_3] = 1.0 \times 10^6$, $[\text{HIO}_2] = 2.0 \times 10^4$, and $[\text{MSA}] = 5.0 \times 10^6$ molec. cm⁻³, indicating that the HIO₂ addition is favorable. To make the readers clear, we accordingly copy the explanation as follows (Lines 235-238 in the revised manuscript): "Furthermore, the effect of HIO₂ addition on the whole nucleation system was considered, as it is not only the rate-limiting step for cluster formation, leading to the significant increasement of the $J(\text{HIO}_3\text{-HIO}_2\text{-MSA})$ compared to $J(\text{HIO}_3\text{-MSA})$ (Figure S12), but also thermodynamically favorable due to HIO₃-HIO₂-MSA path is almost barrierless (1.24 kcal mol⁻¹) compared to HIO₃-MSA pathway (Figure S13)."

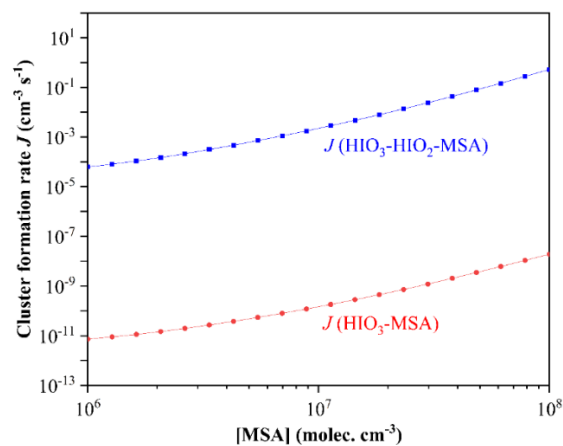


Figure S12. Simulated cluster formation rates J ($\text{cm}^3 \text{s}^{-1}$) against varying $[\text{MSA}] = 10^6 - 10^7$ molec. cm^{-3} , at $T = 278$ K, $\text{CS} = 2.0 \times 10^{-3} \text{ s}^{-1}$, $[\text{HIO}_3] = 1.0 \times 10^6$, $[\text{HIO}_2] = 2.0 \times 10^4$ molec. cm^{-3} .

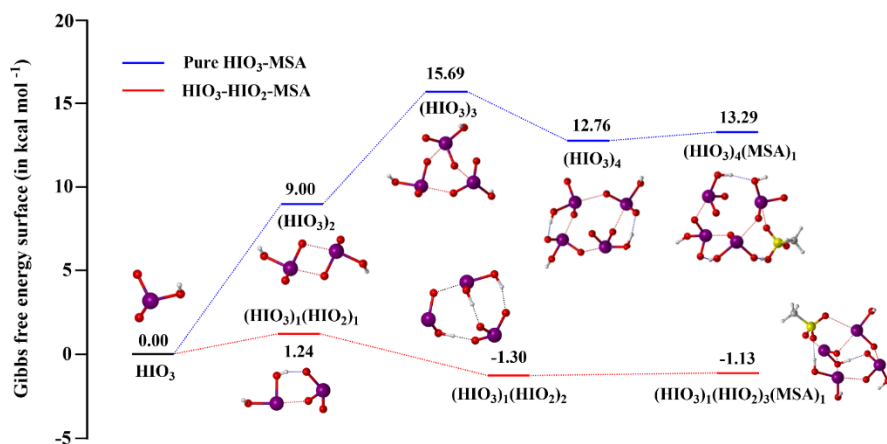


Figure S13. The Gibbs free energies of cluster formation (ΔG , kcal mol^{-1}) based on the main clustering pathway in HIO_3 -MSA and HIO_3 - HIO_2 -MSA nucleation system at $T = 278$ K, $\text{CS} = 2.0 \times 10^{-3} \text{ s}^{-1}$, $[\text{HIO}_3] = 1.0 \times 10^6$, $[\text{HIO}_2] = 2.0 \times 10^4$ molec. cm^{-3} .

Responses to Referee #2's comments

We are grateful to the reviewers for their valuable and helpful comments on our manuscript “**Molecular-level study on the role of methanesulfonic acid in iodine oxoacids nucleation**” (MS No.: egosphere-2023-2084). We have revised the manuscript carefully according to reviewers' comments. The point-to-point responses to the Referee #2's comments are summarized below:

Referee comments:

Jing Li et al. reports a theoretical study on the iodic acid (HIO_3) – iodous acid (HIO_2) based nucleating process enhanced by methanesulfonic acid (MSA) by quantum chemical calculation and cluster dynamic simulation. They found that the MSA can enhance the HIO_3 - HIO_2 -based nucleation, especially in polar oceanic regions. This manuscript has systematically studied the HIO_3 - HIO_2 -MSA ternary nucleation system, covering cluster stability, thermodynamic/kinetic analysis, and molecular-level mechanism. These interesting findings show the significance of sulfur and iodine synergistic nucleation, providing deeper insights into marine secondary particle formation, given chemical complexity of real atmosphere. This well-written manuscript has important atmospheric implications, such as in the studies of marine aerosol formation and the sulfur/iodine cycling. Hence, I recommend the publication of this study in *Atmospheric Chemistry and Physics* after considering my comments listed below.

Response: We appreciate the reviewer for dedicating time to assess our manuscript and providing valuable comments and positive feedback.

General comments:

Comment 1: Although the authors have provided sufficient computational details, it would be better to add the grid settings for DFT calculations and the optimization convergence in method section of the main text.

Response: Based on the reviewer's suggestion, we have added the adopted grid settings (FineGrid) of DFT calculations in Section 2.1 in the main text. Accordingly, the corresponding sentence in Lines 64-65 of page 3 has been restructured as follows: “All density functional

theory (DFT) calculations were carried out using the Gaussian 09 package (Frisch et al., 2009), where FineGrid and tight convergence were employed.”

Comment 2: In general, the nucleation process involves competition between cluster collision and its evaporation processes. In the ACDC simulations presented in this manuscript, could the authors specify which types of collision and evaporation processes considered? If possible, these details would be better to added in the ACDC methodology section.

Response: Thanks. The reviewer's professional comment is beneficial in enhancing the readers' understanding of more simulation details. Accordingly, the detailed settings about the collision and evaporation processes in ACDC simulations have been added in the revised manuscript (Lines 100-102, page 4) as follows: “In the performed ACDC simulations, all possible collision and evaporation processes, including monomer-monomer, monomer-cluster, cluster-cluster collisions, as well as the decomposition of parent clusters into monomers and clusters, or into two smaller clusters, were taken into account.”

Comment 3: In this work, the authors systematically investigated the HIO₃-HIO₂-MSA ternary nucleation process, where HIO₂ appears to play a crucial role in all clustering pathways. How should this be interpreted?

Response: Thanks. It is indeed an important query. As expertly suggested by the reviewer, HIO₂ appears to play a crucial role in all clustering pathways of HIO₃-HIO₂-MSA nucleation. This is mainly because HIO₂, when interacting with acidic HIO₃ or MSA, behaves like base molecules^[9-11]. Specifically, it can serve as a proton acceptor, being protonated by HIO₃ or MSA, leading to the formation of stable acid-base ion pairs. Once HIO₂ is missing, the acid-base reaction between HIO₃ and MSA cannot occur. Thus, HIO₂-induced acid-base reactions with MSA and HIO₃ yield ion pairs whose electrostatic interactions enhance the stability of the formed cluster.

Comment 4: For the formed HIO₃-HIO₂-MSA clusters, especially large-sized clusters, are there any unoccupied binding sites that can enable further molecular binding and cluster growth?

The authors would better provide theoretical evidence by quantum chemical calculations, such as using wave function analysis, or others. If done, this will provide the readers with an intuitive understanding of the growth potential of the cluster.

Response: Following the professional advice of the reviewer, we have performed the electrostatic potential (ESP) analysis for the vacant sites of the stable large-size structure cluster in the revised manuscript. The results of ESP analysis are presented in Fig. S2 below. The red localizations with maximum ESP at the end of the iodine and hydrogen atoms within HIO₃ and HIO₂ along the O–I and O–H direction, which can act as XB or HB donor sites. While the blue regions with minimum ESP of the terminal oxygen atoms have strong nucleophilicity as the HB or XB acceptors.

Herein, we have added the ESP results and analysis to the revised manuscript, and for the convenience of the review, we have copied Figure S2 and the corresponding analysis (Lines 129-132, page 5) as following: “Additionally, taking the (HIO₃)₁(HIO₂)₃(MSA)₁ cluster for example, there are still some potential remaining unoccupied binding sites as shown in Fig. S2. It suggests that the studied large-size clusters still have unoccupied HB and XB sites that can potentially facilitate the condensation of precursors in the atmosphere, enhancing further growth of marine aerosols.”

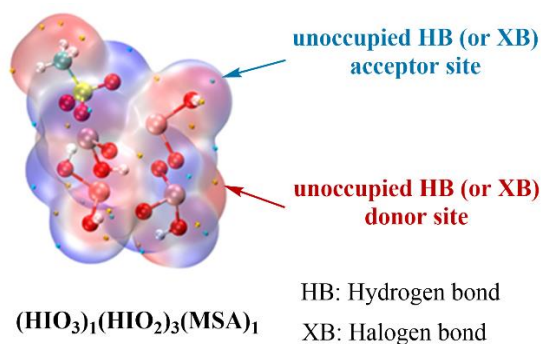


Figure S2. The ESP-mapped molecular vdW surfaces of the (HIO₃)₁(HIO₂)₃(MSA)₁ cluster. The red region is the electron-deficient region, and the blue region is the electron-rich region.

Specific comments:

Comment 5.

Page 3-4, Line 76 and 91: In the equation (2) and (3), the operator $\sum_{i=1}^n N_i, \sum_{j<i} \beta$ should be change to:

$$\sum_{i=1}^n N_i , \quad \sum_{j<i} \beta$$

Response: The operators in the equation (2) and (3) have been corrected accordingly as suggested by the reviewer.

Comment 6.

Page 4, Line 96: Please provide more details of the calculations of the volume of cluster i (V_i).

Response: According to the reviewer's suggestion, the details of the calculations of the volume of cluster i (V_i) have been added in Lines 95-96 (page 4) of the revised manuscript as follows: "And $V_i = 3/4 \times \pi \times (d_i/2)^3$, where the diameter d_i of cluster i is derived from the cluster volume V_i calculated by Multiwfn 3.7."

Comment 7.

Page 5, Figure 1: The authors seem to have forgotten to plot the hydrogen and halogen bonds with dotted lines in Fig. 1(d), please correct it.

Response: Thanks for the reviewer's carefulness. We have added the dotted lines indicating hydrogen and halogen bonds in Fig. 1(d) in the revised manuscript.

Comment 8.

Page 6, Line 141: In the sentence, 'Here, the condensation sink (CS) coefficient is set to be 2.0×10^{-3} ', there is a missing unit after the CS value.

Response: Thanks for the reviewer's careful reading. We have added the missing unit 's⁻¹' after the CS value in the revised manuscript (Line 152, page 6).

Comment 9.

Page 7, Figure 3: To enhance data clarity for readers, consider enlarging the font size in Fig. 3, which appears relatively small.

Response: Based on the reviewer's suggestion, we have adjusted the small font in Fig. 3 in the revised manuscript to enhance content clarity.

Comment 10.

Page 12, Line 252: The word 'play' should be 'plays'.

Response: Accordingly, the word 'play' has been changed to 'plays' in Line 280 of the revised manuscript.

Responses to Referee #3's comments

We are grateful to the reviewers for their valuable and helpful comments on our manuscript “**Molecular-level study on the role of methanesulfonic acid in iodine oxoacids nucleation**” (MS No.: egosphere-2023-2084). We have revised the manuscript carefully according to reviewers' comments. The point-to-point responses to the Referee #3's comments are summarized below:

Referee comments:

This manuscript investigates the enhancement effects of methanesulfonic acid (MSA) on the iodic acid (HIO_3)-iodous acid (HIO_2) nucleation system, which has been reported as an important mechanism of marine new particle formation (NPF). The intermolecular interactions, cluster stability, the formation pathway/ free energy surface of cluster formation as well as the enhancement of formation rate of the HIO_3 - HIO_2 -MSA ternary nucleation system was systematically studied with the combination of quantum chemical simulation and ACDC approach. This paper provided theoretical evidence that the involvement of MSA can structurally stabilize HIO_3 - HIO_2 -based clusters and has positive synergistic effect on the nucleation with HIO_3 and HIO_2 . This manuscript is nicely written and fits the scope of ACP. I recommend the manuscript to be published after the following comments are addressed.

Response: We sincerely thank for the reviewer's careful review of our manuscript, as well as the valuable and positive comments.

General comments:

Comment 1: Although sufficient theoretical details of the cluster conformations have been provided, the authors should also clarify the definition of “stable cluster”. We should derive a cluster's concentration by the competition between its collisional formation and evaporation, instead of only judging the formation free energy. Since the authors have conducted ACDC calculations, the evaporation rates of the major clusters should be discussed, as well as the time dependent concentration variations of these major clusters.

Response: Thanks for the reviewer's professional suggestions. Accordingly, we have added the definition of “stable cluster”, which is determined based on the competition between cluster

collisional formation and evaporation. A cluster is deemed stable when its collisional formation dominates over evaporation^[12]. And the corresponding definition has been added in the revised manuscript (Lines 102-103, page 4) as follows: “Additionally, whether the clusters in the simulated system are stable depends on whether the rate of collision frequencies exceeds the total evaporation rate coefficients ($\beta C/\Sigma\gamma > 1$) (Table S4).”

According to the helpful suggestion of the reviewer, the evaporation rates of the major clusters have been discussed in Lines 175-178 of page 7 as follows: “Generally, stable clusters have lower evaporation rates. According to the calculated cluster evaporation rates ($\Sigma\gamma$, s^{-1}) at 278 K (Table S7), more than 40% of the clusters have $\Sigma\gamma$ less than $10^{-3} s^{-1}$, indicating relatively high stability ($\beta C/\Sigma\gamma > 1$). Among these resulting stable clusters (see Fig. S6), the majority (85%) contains HIO_2 .”

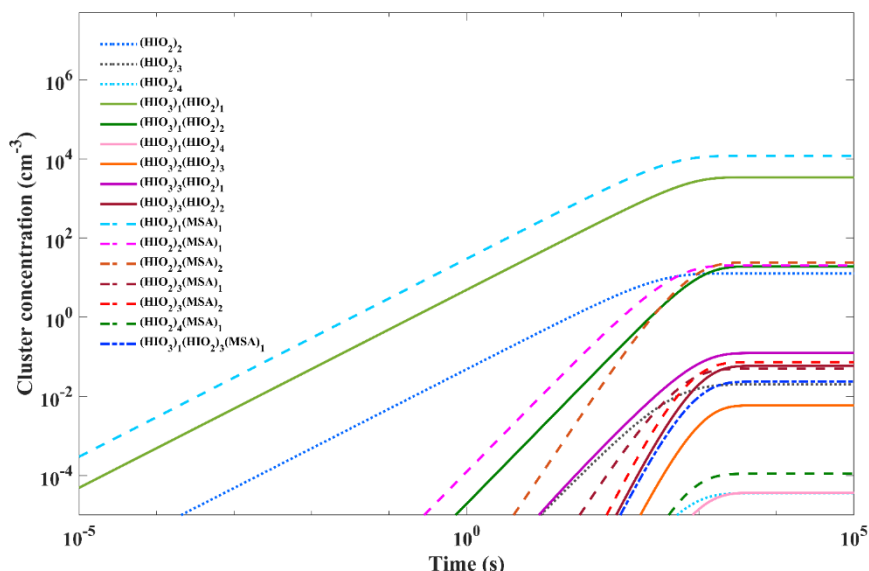


Figure S6. The concentration (molec. cm^{-3}) of stable clusters in HIO_3 - HIO_2 -MSA system as a function of time, at $T = 278$ K, $CS = 2.0 \times 10^{-3} s^{-1}$, $[HIO_3] = 10^6$, $[HIO_2] = 2.0 \times 10^4$, $[MSA] = 5.0 \times 10^6$ molec. cm^{-3} .

Further, as suggested by the reviewer, we calculated the time-dependent concentration variations of the mentioned major cluster sites and presented the simulation results in Fig. S6. The corresponding analysis has been included in the revised manuscript (Line 178-183, page 7), and a copy is provided below: “Moreover, the concentration of these stable clusters increases gradually with time, even reaching a maximum of 10^4 molec. cm^{-3} (Fig. S6). Of these stable clusters, initial $(HIO_3)_1(HIO_2)_1$, $(HIO_2)_2$, and $(MSA)_1(HIO_2)_1$ dimer form rapidly, and at $t = \sim 1$

s, heterotrimers $(\text{HIO}_3)_1(\text{HIO}_2)_2$ and $(\text{MSA})_1(\text{HIO}_2)_2$ begin to form, after which, the larger-sized clusters also form. These time-dependent evidence suggests that MSA is involved in the whole clustering process, from the initial formation of smaller clusters to the large-sized nucleated clusters that potentially further grow.”

Comment 2: I find the results in section 3.2 a bit confusing when trying to interpret the relative importance of the MSA-involved path in HIO_3 - HIO_2 -MSA nucleation under different conditions. For example, Figure 3a (upper panel) shows that the MSA-involved path contributes to 74 % of the cluster formation, under $[\text{MSA}]$ of $5.0 \times 10^6 \text{ molec. cm}^{-3}$, $[\text{HIO}_3]$ of $1.0 \times 10^6 \text{ molec. cm}^{-3}$, while the MSA-involved path contributes to ~20 % under $[\text{MSA}]$ of $1.0 \times 10^6 \text{ molec. cm}^{-3}$, $[\text{HIO}_3]$ of $1.0 \times 10^6 \text{ molec. cm}^{-3}$. This result indicates that MSA is less efficient in clustering with HIO_2 , comparing with HIO_3 . The authors have mentioned the atmospheric concentration level of MSA in line 40, the authors should also include the discussion about the concentration of iodine oxoacids in the revised manuscript. Since if the concentration of HIO_3 is comparable or higher than MSA, the scenario of ACDC simulation cannot reflect the condition of real atmosphere.

Response: Thanks for the reviewer’s insightful comments. As analyzed by the reviewer, MSA exhibits lower efficiency in clustering with HIO_2 compared to HIO_3 . Thus, we agree with the reviewer's suggestion to discuss the conditions with varying iodine oxoacids concentration, as it is very necessary. According to the scenarios presented in Fig. 3(a) (right panel) and Fig. 5 where $[\text{HIO}_3]$ is comparable or higher than $[\text{MSA}]$, the corresponding analyses were supplemented in the revised manuscript (Line 227-231) and copied below: “However, the atmospheric $[\text{HIO}_3]$ ranges widely from 10^6 to $10^8 \text{ molec. cm}^{-3}$. When $[\text{HIO}_3]$ is comparable or higher than $[\text{MSA}]$, the HIO_3 - HIO_2 pathway contributes more, and the R of MSA decreases with the rising $[\text{HIO}_3]$. It is worth noting that when $[\text{HIO}_3]$ is comparable to $[\text{MSA}]$, the R of MSA is greater than 2, as the contribution of MSA to clustering includes not only the direct formation of HIO_3 - HIO_2 -MSA clusters (~20%), but also its ‘catalysis’ role in facilitating formation of initial HIO_3 - HIO_2 clusters (Fig. S7).”

Comment 3: The comparison with field measurements seems to be a bit arbitrary. What's the atmospheric condition such as precursor concentration and temperature of the measurement sites reported? What's the definition of the J in the reported field measurements? Can the reported J be directly compared with the ACDC simulated J ? Moreover, in Line 222, "the observed J of $2.1 \times 10^{-4} \text{ cm}^{-3} \text{ s}^{-1}$ ". This J value is too low for a typical NPF event. Is this value obtained from a non-NPF day? Please check the original paper. More explanation and discussion are needed in this section, which can sharpen the significance of the theoretical study on the merit of atmospheric implication.

Response: Thanks for the reviewer's professional comments.

Item 1) from the reviewer: The comparison with field measurements seems to be a bit arbitrary. What's the atmospheric condition such as precursor concentration and temperature of the measurement sites reported?

Response: (a) Ny-Ålesund: According to Beck^[13] et al., Ny-Ålesund is surrounded by open waters throughout the whole year, with the average annual temperature of -5°C ^[14]. As shown in Figure 1(b) of Beck et al., the ranges of $[\text{HIO}_3]$ and $[\text{MSA}]$ are $10^5 - 10^6$ and $10^6 - 10^8$ molec. cm^{-3} , respectively. And the author mentioned that "An explanation for this could be the very low condensation sink of $\sim 4 \times 10^{-4} \text{ s}^{-1}$ at Ny-Ålesund...".

Thus, the simulation conditions were set to: $T = 268 \text{ K}$, $\text{CS} = 4.0 \times 10^{-4} \text{ s}^{-1}$, $[\text{HIO}_3] = 10^5 - 10^6$, $[\text{HIO}_2] = 2.0 \times 10^3 - 2.0 \times 10^4$, and $[\text{MSA}] = 10^6 - 10^8$ molec. cm^{-3} .

(b) Marambio: According to the description of Marambio^[15], many sunny days are observed, occurring with ambient temperatures above 0°C . The author mentioned that the measured gas-phase concentrations of the species of interest showed maxima of $\sim 2.3 \times 10^7$, and $\sim 3.6 \times 10^6$ molecules cm^{-3} for the total MSA and HIO_3 concentration, respectively.

Combined with the ranges of $[\text{HIO}_3]$ and $[\text{MSA}]$ from Figures 5 and 6 in the original paper describing Marambio^[15], thus, the simulation conditions were set to: $T = 273 \text{ K}$, $\text{CS} = 1.0 \times 10^{-4} \text{ s}^{-1}$, $[\text{HIO}_3] = 10^5 - 10^6$, $[\text{HIO}_2] = 2.0 \times 10^3 - 2.0 \times 10^4$, and $[\text{MSA}] = 10^6 - 10^7$ molec. cm^{-3} .

(c) Mace Head: In Mace Head, the concentration of HIO_3 during the new particle formation events reached 10^8 molecules cm^{-3} , and the range of $[\text{HIO}_3]$ is set to $10^6 - 10^8$ molec. cm^{-3} according to Figure 1(b) ^[6]. Moreover, Berresheim et al. reported that the range of $[\text{MSA}]$ is $10^5 - 10^7$ molec. cm^{-3} , and the temperature can reach to 14°C , as shown in Figure 6 ^[16].

Thus, the simulation conditions were set to: $T = 287$ K, $CS = 2.0 \times 10^{-3} \text{ s}^{-1}$, $[\text{HIO}_3] = 10^7 - 10^8$, $[\text{HIO}_2] = 2.0 \times 10^5 - 2.0 \times 10^6$, and $[\text{MSA}] = 10^6 - 10^7 \text{ molec. cm}^{-3}$.

(d) Réunion: According to Salignat et al., the average $[\text{HIO}_3]$ is $2.90 \times 10^5 \text{ molec. cm}^{-3}$, and the ranges of $[\text{HIO}_3]$ and $[\text{MSA}]$ are $10^5 - 10^7$ and $10^6 - 10^7 \text{ molec. cm}^{-3}$, respectively, according to Figure 8(a) in the original paper about Réunion^[17]. As shown in Figure 4(a), the temperature ranges from 10 to 20 °C.

Thus, the simulation conditions were set to: $T = 288$ K, $CS = 2.0 \times 10^{-3} \text{ s}^{-1}$, $[\text{HIO}_3] = 10^5 - 3.0 \times 10^6$, $[\text{HIO}_2] = 2.0 \times 10^3 - 6.0 \times 10^4$, and $[\text{MSA}] = 10^6 - 10^8 \text{ molec. cm}^{-3}$.

Item 2) from the reviewer: What's the definition of the J in the reported field measurements? Can the reported J be directly compared with the ACDC simulated J ?

Response: In the ACDC simulation, nucleation generally refers to the formation of relatively stable clusters for which collisions with molecules can be assumed to dominate over cluster evaporation. Accordingly, the cluster formation rate (J) indicates the particle flux out of the studied system. In this case, it is the rate of clusters forming at some specific size (*i.e.* the net flux into the size from all other sizes)^[12]. In field observation, the formation rates ($J_{1.5}$) were measured by instruments, such as nitrate chemical ionization atmospheric pressure interface Time-Of-Flight mass spectrometer (CI-APi-TOF)^[13], differential mobility particle sizer (DMPS) and neutral cluster and air ion spectrometer (NAIS)^[15].

According to the Kerminen-Kulmala equation^[18], cluster formation rates for d_2 nm clusters (J_{d_2}) relate to those for d_1 nm clusters (J_{d_1}) by

$$J_{d_1} = J_{d_2} \exp \left\{ \gamma \left(\frac{1}{d_1} - \frac{1}{d_2} \right) \frac{CS}{GR_{d_2-d_1}} \right\}$$

where the $GR_{d_2-d_1}$ is the initial cluster growth rate from d_1 to d_2 nm, and CS represents condensation sink of clusters by preexisting particles. The parameter γ depends on many factors but can usually be approximated by assuming it to be equal to $0.23 \text{ nm}^2 \text{ m}^2 \text{ h}^{-1}$.

In this study, the relationship between the formation rates of simulated clusters ($J_{1.2}$) and that of observed clusters ($J_{1.5}$) can be written as:

$$J_{1.2} = J_{1.5} \exp \left\{ 0.23 \times \left(\frac{1}{1.2} - \frac{1}{1.5} \right) \frac{CS}{GR} \right\}$$

where GR was measured to be $3.2 - 4.4 \text{ nm} \cdot \text{h}^{-1}$ in the $1.1 - 2.0 \text{ nm}$ size range during three observed events^[2, 19], and CS was 0.002 s^{-1} . $J_{1.2}$ was then calculated to be $1.00001 - 1.00002$

times of $J_{1.5}$. Thus, the observed cluster formation rates for 1.5 nm clusters can be directly comparable with the simulated $J_{1.2}$.

We have included corresponding justification in Section 3.4 of the revised manuscript (Lines 242-243, Page 11) and supporting file as follows: “Subsequently, we compared these simulation results with observed nucleation rates and the definition of cluster formation rate was detailed in Supporting Information (SI).”

Item 3) from the reviewer: Moreover, in Line 222, “the observed J of $2.1 \times 10^{-4} \text{ cm}^{-3} \text{ s}^{-1}$ ”. This J value is too low for a typical NPF event. Is this value obtained from a non-NPF day? Please check the original paper.

Response: Following the reviewer’s suggestion, we have carefully checked the original paper. According to the captions of Fig. 2 (“Examples representing seasonal behavior of NPF observed at Villum and Ny-Ålesund”)^[13], the present J of $2.1 \times 10^{-4} - 10^{-1} \text{ cm}^{-3} \text{ s}^{-1}$ (Figure 2 (c5)) originate from the observed NPF data values during May 4, 2017. Notably, as professionally judged by the reviewer, Beck et al. have also clarified that data with J -values $<$ a few $10^{-3} \text{ cm}^{-3} \text{ s}^{-1}$ (including the mentioned lower J of $2.1 \times 10^{-4} \text{ cm}^{-3} \text{ s}^{-1}$) are highly unreliable and reflect mainly the noise levels^[13]. And thus, these low and uncertain J values hardly correspond to NPF events.

Therefore, we have adjusted the range of the observed J of Ny-Ålesund to a reliable range of $10^{-3} - 10^{-1} \text{ cm}^{-3} \text{ s}^{-1}$ in Fig. 6(a). Meanwhile, the related statement “...the $J(\text{HIO}_3\text{-HIO}_2\text{-MSA})$ can be two orders of magnitude higher than the observed J of $2.1 \times 10^{-4} \text{ cm}^{-3} \text{ s}^{-1}$ ” has been changed to “...the $J(\text{HIO}_3\text{-HIO}_2\text{-MSA})$ can be one order of magnitude higher than the observed J of $10^{-3} \text{ cm}^{-3} \text{ s}^{-1}$ ” in Lines 248-249 (page 11) of the revised manuscript.

Specific comments:

Comment 4: It would be preferable to avoid including reference in the abstract.

Response: The reference in the abstract has been removed in the revised manuscript.

Comment 5: Abbreviations such as ESP HB XB should be explained at least once in the main text.

Response: Thanks for the reviewer's careful reading, all the abbreviations, such as ESP (Electrostatic potential), HB (Hydrogen bond) and XB (Halogen bond), have been explained in their first appearance in the revised manuscript.

Comment 6: Line 47, " Furthermore, given the coexistence of MSA and HIO₃ in different marine regions (Quéléver et al., 2022; Beck et al., 2021), the HIO₃-HIO₂-MSA nucleating mechanism may differ under distinct ambient conditions, but it remains unrevealed." First, nucleating should be nucleation. Second, I feel a bit confusion about this sentence. Is the different HIO₃/MSA and HIO₂/MSA concentration ratio leads to different nucleation mechanism? The authors have concluded that MSA can promote nucleation, particularly in marine regions characterized by lower T, lower [HIO₃] and [HIO₂]. It will be more preferable to add some discussion about the [HIO₃]/ [HIO₂] in different marine atmosphere.

Response: Thanks for the reviewer's helpful comments.

Item 1) from the reviewer: Line 47, " Furthermore, given the coexistence of MSA and HIO₃ in different marine regions (Quéléver et al., 2022; Beck et al., 2021), the HIO₃-HIO₂-MSA nucleating mechanism may differ under distinct ambient conditions, but it remains unrevealed." First, nucleating should be nucleation.

Response: As suggested by the reviewer, all 'nucleating' have been changed to 'nucleation' in the revised manuscript.

Item 2) from the reviewer: Second, I feel a bit confusion about this sentence. Is the different HIO₃/MSA and HIO₂/MSA concentration ratio leads to different nucleation mechanism?

Response: As to the mentioned sentence, in fact, here we would like to express that the dominant nucleation mechanism varies with the region. Accordingly, we have rephrased the sentence (Lines 46-48) as follows: "Furthermore, given the coexistence of MSA and HIO₃ in different marine regions (Quéléver et al., 2022; Beck et al., 2021), along with the consistent presence of HIO₃ and HIO₂ as homologous substances^[6], the importance of the HIO₃-HIO₂-MSA nucleation mechanism may differ under distinct ambient conditions, due to their uneven distribution, but it remains unrevealed."

Item 3) from the reviewer: The authors have concluded that MSA can promote nucleation, particularly in marine regions characterized by lower T , lower $[\text{HIO}_3]$ and $[\text{HIO}_2]$. It will be more preferable to add some discussion about the $[\text{HIO}_3]/[\text{HIO}_2]$ in different marine atmosphere.

Response: Furthermore, according to the reviewer's suggestion, we have added the discussion about $[\text{HIO}_3]/[\text{HIO}_2]$ in the revised manuscript (Lines 224-226, page 10) as follows: "Furthermore, at the conditions with lower $[\text{HIO}_3]/[\text{HIO}_2]$, where R is higher, the contribution of MSA nucleation with HIO_2 increase due to the relative scarcity of HIO_3 . Conversely, R decreases at higher $[\text{HIO}_3]/[\text{HIO}_2]$, i.e., the impacts of MSA decreases."

Comment 7: More explanation of ACDC model setting is needed. For example, the setting of condensation sink and other model parameters.

Response: Thanks for reviewer's valuable suggestions. The model parameters in the performed ACDC simulations include: condensation sink (CS), temperature (T), precursor concentrations, boundary clusters, collision/evaporation processes (monomer-monomer, monomer-cluster, cluster-cluster). Concerning all the ACDC simulation data presentation, the settings of T , CS , and precursor concentrations were provided in the main text and figure captions. And the details on boundary clusters and the employed collision/evaporation processes were added in the Tables S3, S5, and S6 of the Supplementary Information.

Comment 8: Figure 6. The HIO_3 - HIO_2 curve should be an area as the other two.

Response: Thanks. The reviewer's comment is important for the clear presentation of the data. Here, we present the rate of HIO_3 - HIO_2 nucleation as a line in Fig. 6, due to the setting of the fixed $[\text{HIO}_3]/[\text{HIO}_2]$ in the simulation, given the homology of HIO_3 and HIO_2 , as well as their reported concentration ratio^[6]. To avoid potential confusion for readers, we clarified the association between $[\text{HIO}_3]$ and $[\text{HIO}_2]$ in the caption of Fig. 6, stating: " $[\text{HIO}_3]/[\text{HIO}_2]$ is a constant".

Comment 9: It would be preferable to include some uncertainty analysis.

Response: Thanks, this is an important point to improve the robustness of the results. The potential uncertainties may arise from ACDC simulations and quantum chemical (QC)

calculations, thereby we examined how variable ACDC settings, such as condensation sink coefficient (CS), sticking factor (SF, corresponding to a sticking probability for cluster/monomer collision) and the change of calculated Gibbs free energy of cluster formation (ΔG , from quantum chemical calculations) impact the enhancement of MSA (R_{MSA}) on cluster formation rate (J). Here, the CS values ranged from $1.0 \times 10^{-4} \text{ s}^{-1}$ to $1.0 \times 10^{-2} \text{ s}^{-1}$, covering possible CS in relatively clean and polluted regions^[1, 2]. The range of SF was set from 0.1 to 1.0 since sticking probabilities for neutral-neutral collisions between 0.1 and 1.0^[3].

As shown in the Figs. S15 (a) and (b), although both CS and SF affect R_{MSA} to some extent, the uncertainty range are relatively limited (CS < 32.5% and SF < 17.1%) and the results does not affect the trend and main conclusions.

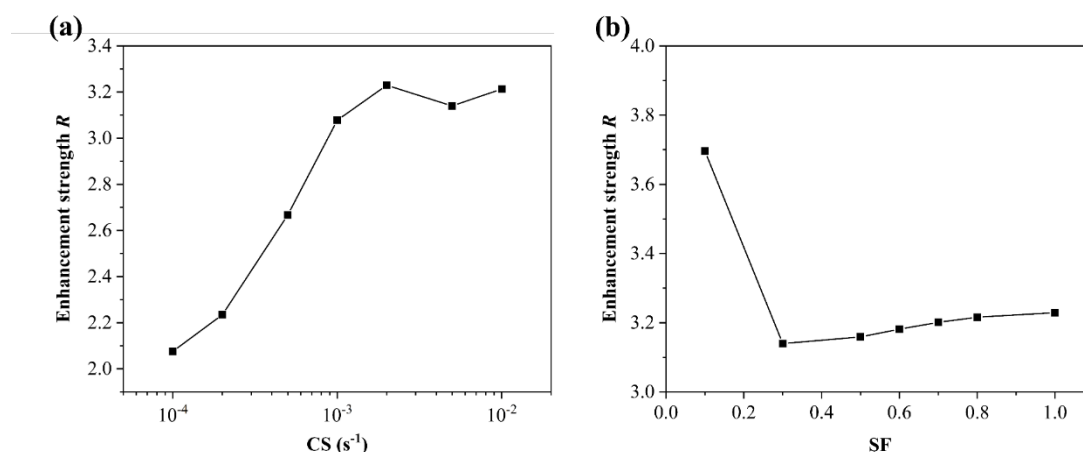


Figure S15. Variation of enhancement strength R of MSA with (a) condensation sink coefficient (CS) and (b) sticking factor (SF) for $\text{HIO}_3\text{-HIO}_2\text{-MSA}$ system at $T = 278 \text{ K}$, $[\text{HIO}_3] = 1.0 \times 10^7$, $[\text{HIO}_2] = 2.0 \times 10^5$, and $[\text{MSA}] = 1.0 \times 10^7 \text{ molec. cm}^{-3}$.

In addition, the potential uncertainty of quantum chemical calculations is ultimately manifested in the calculated ΔG values. As reported by Kupiainen^[4] et al. (2012), the differences between the computational (DFT//RI-CC2 method) and experimental ΔG values are about 1 kcal mol^{-1} or less^[5]. Accordingly, Almedia^[3] et al. (2013) calculated the uncertainty range of ACDC simulated cluster formation resulting from QC calculations by adjusting the binding energy ($\pm 1 \text{ kcal mol}^{-1}$). Further given the consistency of our research framework (DFT//RI-CC2 + ACDC) with Almedia et al. (2013), herein we have performed the uncertainty analysis of R_{MSA} caused by QC calculations through adding or subtracting 1 kcal mol^{-1} from the ΔG (using $\Delta G_{278\text{K}}$ as a reference). The figure below presents the uncertainty analysis results of

J and R_{MSA} at $T = 278$ K, $\text{CS} = 2.0 \times 10^{-3} \text{ s}^{-1}$, $[\text{HIO}_3] = 10^7$, $[\text{HIO}_2] = 2.0 \times 10^5$, $[\text{MSA}] = 10^6 - 10^8 \text{ molec. cm}^{-3}$.

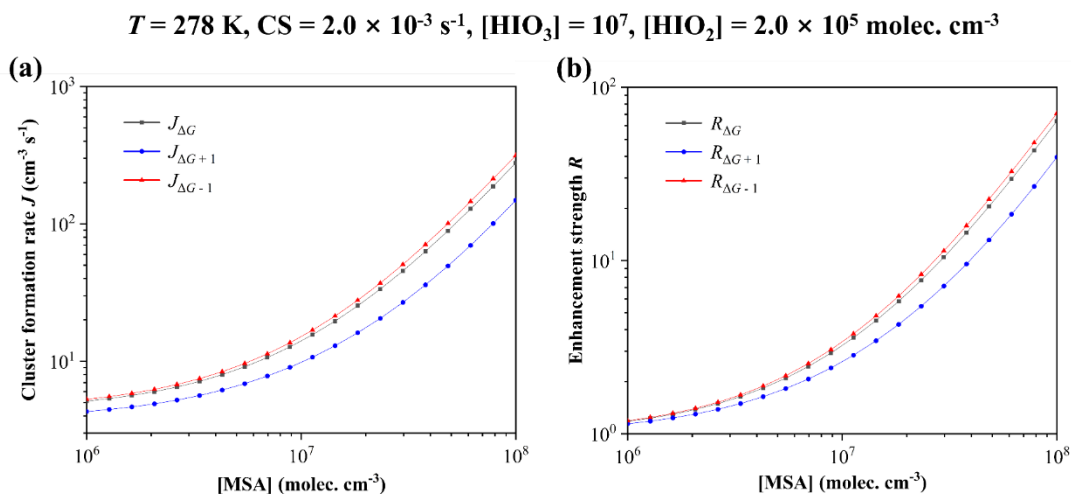


Figure S16. Cluster formation rate J (a) and enhancement strength R of MSA (b) as a function of $[\text{MSA}] = 10^6 - 10^8 \text{ molec. cm}^{-3}$, with different energy of $\Delta G_{278\text{K}}$ (black line), $\Delta G_{278\text{K}} + 1$ (blue line), $\Delta G_{278\text{K}} - 1$ (red line), at $T = 278$ K, $\text{CS} = 2.0 \times 10^{-3} \text{ s}^{-1}$, $[\text{HIO}_3] = 10^7$, $[\text{HIO}_2] = 2.0 \times 10^5 \text{ molec. cm}^{-3}$.

Here, we have added the results of R_{MSA} under different CS, SF and ΔG to the revised supporting file, and for the convenience of the review, we have copied Figures S15-S16 and the corresponding analysis as following: “Here, the potential uncertainties may stem from ACDC simulations and quantum chemical (QC) calculations, we examined the effect of condensation sink coefficient (CS), sticking factor (SF) and calculated ΔG of clusters on enhancement of MSA to the cluster formation rate. The CS values ranged from $1.0 \times 10^{-4} \text{ s}^{-1}$ to $1.0 \times 10^{-2} \text{ s}^{-1}$, covering possible CS in relatively clean and polluted regions^[1, 2]. The range of SF was set from 0.1 to 1.0 since sticking probabilities for neutral-neutral collisions between 0.1 and 1.0^[3]. Both the CS and SF slightly affect the enhancement of MSA, with limited uncertainty range of $\text{CS} < 32.5\%$ and $\text{SF} < 17.1\%$ (Fig. S15). As reported by Kupiainen^[4] et al. (2012), the differences between the computational (DFT//RI-CC2 method) and experimental ΔG values are about 1 kcal mol^{-1} or less^[5]. Accordingly, Almedia^[3] et al. (2013) calculated the uncertainty range of ACDC simulated cluster formation resulting from QC calculations by adjusting the binding energy ($\pm 1 \text{ kcal mol}^{-1}$). Further given the consistency of our research framework (DFT//RI-CC2 + ACDC) with Almedia et al. (2013), herein we have performed the uncertainty

analysis of R_{MSA} caused by QC calculations through adding or subtracting 1 kcal mol^{-1} from the ΔG (using $\Delta G_{278\text{K}}$ as a reference). As shown in Table S8 and Fig. S16, adjusting the $\Delta G_{278\text{K}}$ of clusters by $\pm 1 \text{ kcal mol}^{-1}$ resulted in a minor variation in J and R of MSA, with the overall trend remaining consistent.”

Responses to Referee #4's comments

We sincerely appreciate the reviewer's valuable and helpful comments on our manuscript "**Molecular-level study on the role of methanesulfonic acid in iodine oxoacids nucleation**" (MS No.: egosphere-2023-2084). We have revised the manuscript carefully according to reviewer's comments. The point-to-point responses to the Referee #4's comments are summarized below:

Referee comments:

This manuscript explores the enhancement effects of MSA on the HIO₃-HIO₂ system through DFT calculations and kinetic analysis. It is found that adding MSA significantly enhances the nucleation rate, especially in colder regions. The calculations are also compared with observations and in general the MSA-HIO₃-HIO₂ nucleation better explains the results than the binary HIO₃-HIO₂ nucleation. Overall, I find this manuscript clearly written and it is a nice contribution to the literature. The manuscript can be published after the following comments are addressed.

Response: We would like to thank the reviewer for taking the time to review our manuscript and for providing the professional comments and positive feedback.

Major comments:

Comment 1: What is the criterion for stable clusters (based on which nucleation rates can be defined)? Are they determined based on the growth rate/dissociation rate ratio? A clear definition should be given in the main text.

Response: Indeed, as expertly suggested by the reviewer, whether a cluster is stable or not is determined based on the cluster growth rate/dissociation rate ratio. In ACDC simulations^[20], stable clusters are those in which collisions with molecules can be assumed to dominate over cluster evaporation.

According to the reviewer's helpful suggestions, the corresponding definition has been added in the main text of the revised manuscript (Lines 102-103, Page 4) as follows: "Additionally, whether the clusters in the simulated system are stable depends on whether the rate of collision frequencies exceeds the total evaporation rate coefficients ($\beta C/\Sigma\gamma > 1$) (Table

S4).”

Comment 2: Section 3.4: how J is defined/calculated in the measurements should be discussed here, since I assume it is different from the definition used in the simulation. In other words, more justification of why the simulated rates and observed rates are directly comparable should be provided.

Response: This is a very helpful point – thanks for bringing it up. In the ACDC simulation, nucleation generally refers to the formation of relatively stable clusters for which collisions with molecules can be assumed to dominate over cluster evaporation. Accordingly, the cluster formation rate (J) indicates the particle flux out of the studied system. In this case, it is the rate of clusters forming at some specific size (*i.e.* the net flux into the size from all other sizes)^[12]. In field observation, the formation rates ($J_{1.5}$) were measured by instruments, such as nitrate chemical ionization atmospheric pressure interface Time-Of-Flight mass spectrometer (CI-API-TOF)^[13], differential mobility particle sizer (DMPS) and neutral cluster and air ion spectrometer (NAIS)^[15].

According to the Kerminen-Kulmala equation ^[18], cluster formation rates for d_2 nm clusters (J_{d_2}) relate to those for d_1 nm clusters (J_{d_1}) by

$$J_{d_1} = J_{d_2} \exp \left\{ \gamma \left(\frac{1}{d_1} - \frac{1}{d_2} \right) \frac{CS}{GR_{d_2-d_1}} \right\},$$

where the $GR_{d_2-d_1}$ is the initial cluster growth rate from d_1 to d_2 nm, and CS represents condensation sink of clusters by preexisting particles. The parameter γ depends on many factors but can usually be approximated by assuming it to be equal to $0.23 \text{ nm}^2 \text{ m}^2 \text{ h}^{-1}$.

In this study, the relationship between the formation rates of simulated clusters ($J_{1.2}$) and that of observed clusters ($J_{1.5}$) can be written as:

$$J_{1.2} = J_{1.5} \exp \left\{ 0.23 \times \left(\frac{1}{1.2} - \frac{1}{1.5} \right) \frac{CS}{GR} \right\},$$

where GR was measured to be $3.2 - 4.4 \text{ nm} \cdot \text{h}^{-1}$ in the $1.1 - 2.0 \text{ nm}$ size range during three observed events^[2, 19], and CS was 0.002 s^{-1} . $J_{1.2}$ was then calculated to be $1.00001 - 1.00002$ times of $J_{1.5}$. Thus, the observed cluster formation rates for 1.5 nm clusters can be directly comparable with the simulated $J_{1.2}$.

We have included corresponding justification in Section 3.4 of the revised manuscript

(Lines 242-243, Page 11) and supporting file as follows: “Subsequently, we compared these simulation results with observed nucleation rates and the definition of cluster formation rate was detailed in Supporting Information (SI).”

Comment 3: I suggest the authors do two types of calculations corresponding to polluted (CS larger than 0.002/s) and relatively clean environments. This could benefit future research in more polluted coastal regions.

Response: Thanks, these suggestions from the reviewer are very important for improving the environmental impacts of the HIO₃-MSA-HIO₂ nucleation. Accordingly, we have performed additional ACDC simulations with CS values of $1.0 \times 10^{-2} \text{ s}^{-1}$ and $1.0 \times 10^{-4} \text{ s}^{-1}$ corresponding to polluted and relatively clean environments, respectively. The figures below present the results of the simulated cluster formation rates J (Figures S8-S9) and enhancement strength R of MSA (Figures S10-S11).

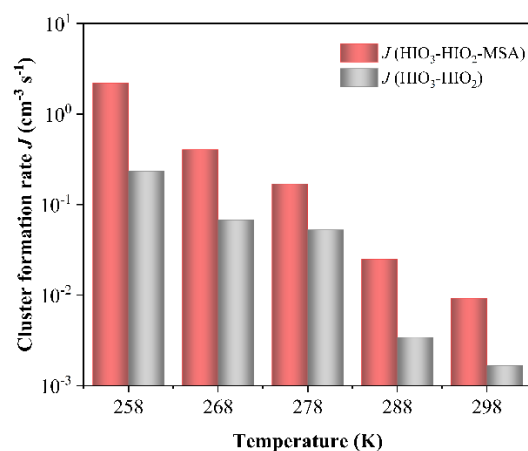


Figure S8. Simulated cluster formation rates J ($\text{cm}^{-3} \text{ s}^{-1}$) against varying atmospheric temperatures ($T = 258 - 298 \text{ K}$), $\text{CS} = 1.0 \times 10^{-2} \text{ s}^{-1}$, $[\text{HIO}_3] = 1.0 \times 10^7$, $[\text{HIO}_2] = 2.0 \times 10^5$, and $[\text{MSA}] = 1.0 \times 10^7 \text{ molec. cm}^{-3}$.

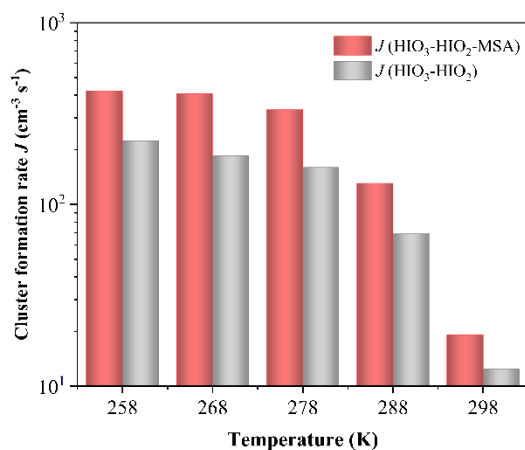


Figure S9. Simulated cluster formation rates J ($\text{cm}^{-3} \text{s}^{-1}$) against varying atmospheric temperatures ($T = 258 - 298 \text{ K}$), $\text{CS} = 1.0 \times 10^{-4} \text{ s}^{-1}$, $[\text{HIO}_3] = 1.0 \times 10^7$, $[\text{HIO}_2] = 2.0 \times 10^5$, and $[\text{MSA}] = 1.0 \times 10^7 \text{ molec. cm}^{-3}$.

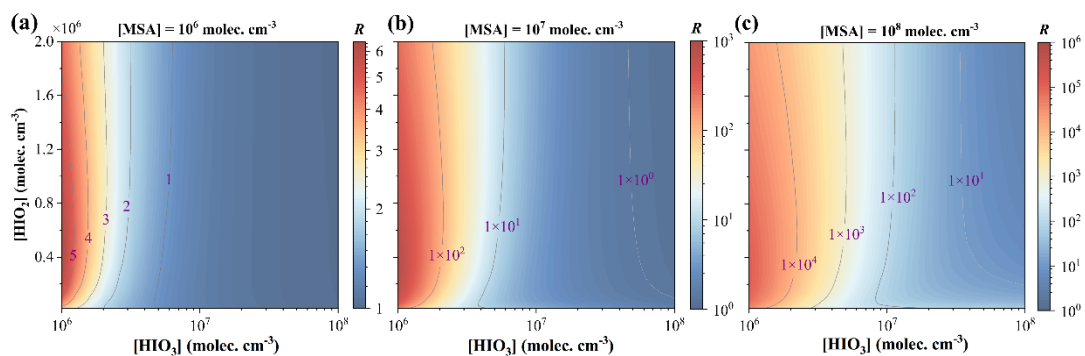


Figure S10. Enhancement strength R of MSA on cluster formation rates at varying precursor concentrations: $[\text{HIO}_3] = 10^6 - 10^8$, $[\text{HIO}_2] = 2.0 \times 10^4 - 2.0 \times 10^6 \text{ molec. cm}^{-3}$, (a) $[\text{MSA}] = 1.0 \times 10^6 \text{ molec. cm}^{-3}$, (b) $[\text{MSA}] = 1.0 \times 10^7 \text{ molec. cm}^{-3}$, and (c) $[\text{MSA}] = 1.0 \times 10^8 \text{ molec. cm}^{-3}$, $T = 278 \text{ K}$, $\text{CS} = 1.0 \times 10^{-2} \text{ s}^{-1}$.

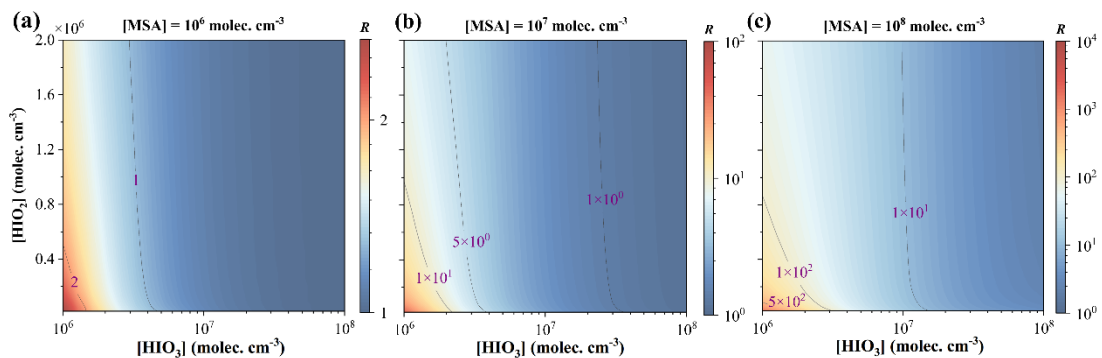


Figure S11. Enhancement strength R of MSA on cluster formation rates at varying precursor

concentrations: $[\text{HIO}_3] = 10^6 - 10^8$, $[\text{HIO}_2] = 2.0 \times 10^4 - 2.0 \times 10^6$ molec. cm^{-3} , **(a)** $[\text{MSA}] = 1.0 \times 10^6$ molec. cm^{-3} , **(b)** $[\text{MSA}] = 1.0 \times 10^7$ molec. cm^{-3} , and **(c)** $[\text{MSA}] = 1.0 \times 10^8$ molec. cm^{-3} , $T = 278$ K, $\text{CS} = 1.0 \times 10^{-4} \text{ s}^{-1}$.

Herein, we have added the simulated J and R results, along with their analysis, in the revised supporting file (Figures S8 – S11). For the convenience of the review, we have copied the corresponding analysis (Lines 233-235, Page 10) as following: “In addition, we also examined the conditions in relatively polluted ($\text{CS} = 1.0 \times 10^{-2} \text{ s}^{-1}$) and clean environments ($\text{CS} = 1.0 \times 10^{-4} \text{ s}^{-1}$) and found that, similar to the environment with CS value of $2.0 \times 10^{-3} \text{ s}^{-1}$, MSA exhibits significant promoting effects on iodine particle formation (Figs. S8-S11).”

Comment 4: Figure 6. I believe the blue line should be an area as the other two. Also, how does the rates differ if the uncertainties of the DFT calculations for key clusters are considered? A table might be provided for this uncertainty analysis.

Response: We appreciate the insightful and rigorous comments from the reviewer. These suggestions can enhance the robustness of the simulation results. The blue line in Fig. 6 depicts HIO_3 - HIO_2 nucleation rate, and since the ratio $[\text{HIO}_3]/[\text{HIO}_2]$ is held constant (50) according to the measured ratio $\text{HIO}_3/\text{HIO}_2$ from Sipilä et al. 2016^[6], resulting in a line increasing with HIO_3 concentration. We have added description of the relationship between $[\text{HIO}_3]$ and $[\text{HIO}_2]$ to the caption of Figure 6 as: “[HIO_3]/[HIO_2] is a constant”. Therefore, as $[\text{HIO}_3]$ increases, the $J(\text{HIO}_3\text{-HIO}_2)$ does change as a line.

In addition, following the expert advice of the reviewer, we examined the effects of DFT computational uncertainty for key clusters on the rate as well as on the enhancement R of MSA . The uncertainties of the DFT calculations ultimately manifested in the calculated ΔG values. As reported by Kupiainen^[4] et al. (2012), the differences between the computational (DFT//RI-CC2 method) and experimental ΔG values are about 1 kcal mol^{-1} or less^[5]. Accordingly, Almedia^[3] et al. (2013) calculated the uncertainty range of ACDC simulated cluster formation resulting from QC calculations by adjusting the binding energy ($\pm 1 \text{ kcal mol}^{-1}$). Further given the consistency of our research framework (DFT//RI-CC2 + ACDC) with Almedia et al. (2013), herein we have performed the uncertainty analysis of R_{MSA} caused by QC calculations through adding or subtracting 1 kcal mol^{-1} from the ΔG (using $\Delta G_{278\text{K}}$ as a reference). The table and

figure below present the uncertainty analysis results of J and R_{MSA} at $T = 278$ K, $\text{CS} = 2.0 \times 10^{-3} \text{ s}^{-1}$, $[\text{HIO}_3] = 10^7$, $[\text{HIO}_2] = 2.0 \times 10^5$, $[\text{MSA}] = 10^6 - 10^8 \text{ molec. cm}^{-3}$.

Table S8. Cluster formation rate J of HIO_3 - HIO_2 - MSA system under different Gibbs free energy ($\Delta G_{278\text{K}}$, $\Delta G_{278\text{K}} + 1$, $\Delta G_{278\text{K}} - 1$) at $T = 278$ K, $\text{CS} = 2.0 \times 10^{-3} \text{ s}^{-1}$, $[\text{HIO}_3] = 10^7$, $[\text{HIO}_2] = 2.0 \times 10^5$, $[\text{MSA}] = 10^6 - 10^8 \text{ molec. cm}^{-3}$.

[MSA]	$J_{\Delta G}$	$J_{\Delta G-1}$	$J_{\Delta G+1}$
1.00×10^6	5.13×10^0	4.31×10^0	5.29×10^0
1.27×10^6	5.35×10^0	4.46×10^0	5.53×10^0
1.62×10^6	5.64×10^0	4.65×10^0	5.84×10^0
2.07×10^6	6.01×10^0	4.90×10^0	6.25×10^0
2.64×10^6	6.50×10^0	5.22×10^0	6.78×10^0
3.36×10^6	7.14×10^0	5.63×10^0	7.47×10^0
4.28×10^6	7.99×10^0	6.17×10^0	8.40×10^0
5.46×10^6	9.12×10^0	6.87×10^0	9.64×10^0
6.95×10^6	1.06×10^1	7.80×10^0	1.13×10^1
8.86×10^6	1.27×10^1	9.04×10^0	1.36×10^1
1.13×10^7	1.56×10^1	1.07×10^1	1.68×10^1
1.44×10^7	1.96×10^1	1.30×10^1	2.14×10^1
1.83×10^7	2.53×10^1	1.61×10^1	2.78×10^1
2.34×10^7	3.35×10^1	2.05×10^1	3.71×10^1
2.98×10^7	4.55×10^1	2.68×10^1	5.07×10^1
3.79×10^7	6.31×10^1	3.60×10^1	7.08×10^1
4.83×10^7	8.93×10^1	4.95×10^1	1.01×10^2
6.16×10^7	1.29×10^2	6.98×10^1	1.46×10^2
7.85×10^7	1.88×10^2	1.01×10^2	2.13×10^2
1.00×10^8	2.78×10^2	1.49×10^2	3.15×10^2

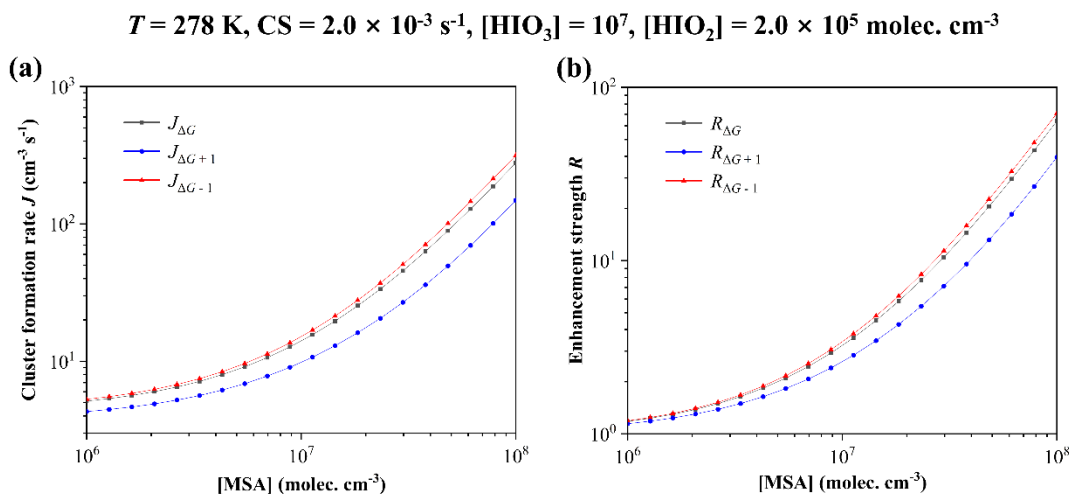


Figure S16. Cluster formation rate J (a) and enhancement strength R of MSA (b) as a function of $[\text{MSA}] = 10^6 - 10^8 \text{ molec. cm}^{-3}$, with different energy of $\Delta G_{278\text{K}}$ (black line), $\Delta G_{278\text{K}} + 1$ (blue line), $\Delta G_{278\text{K}} - 1$ (red line), at $T = 278 \text{ K}$, $CS = 2.0 \times 10^{-3} \text{ s}^{-1}$, $[\text{HIO}_3] = 10^7$, $[\text{HIO}_2] = 2.0 \times 10^5 \text{ molec. cm}^{-3}$.

For the convenience of the review, we have copied Table S8 and Figure S16 and the corresponding analysis (in the revised supporting file) as following: “As reported by Kupiainen^[4] et al. (2012), the differences between the computational (DFT//RI-CC2 method) and experimental ΔG values are about 1 kcal mol^{-1} or less^[5]. Accordingly, Almedia^[3] et al. (2013) calculated the uncertainty range of ACDC simulated cluster formation resulting from QC calculations by adjusting the binding energy ($\pm 1 \text{ kcal mol}^{-1}$). Further given the consistency of our research framework (DFT//RI-CC2 + ACDC) with Almedia et al. (2013), herein we have performed the uncertainty analysis of R_{MSA} caused by QC calculations through adding or subtracting 1 kcal mol^{-1} from the ΔG (using $\Delta G_{278\text{K}}$ as a reference). As shown in Table S8 and Fig. S16, adjusting the $\Delta G_{278\text{K}}$ of clusters by $\pm 1 \text{ kcal mol}^{-1}$ resulted in a minor variation in J and R of MSA, with the overall trend remaining consistent.”

Technical comments:

Comment 5: Line 24: nucleating -> nucleation. This replacement should be done in several places in the text.

Response: Thanks for this helpful comment., the “nucleating” has been changed to “nucleation” in the revised manuscript.

Comment 6: Line 27: remove the second comma.

Response: The second comma has been removed in the revised manuscript.

Comment 7: Line 35: might be rewritten as: Although the efficient nucleation of HIO₃ and HIO₂ is overall consistent with the CLOUD measurements, this mechanism does not account for all HIO₃-induced nucleation in the real atmosphere.

Response: Thanks, the wording suggested by the reviewer is more appropriate. Accordingly, the sentence has been rewritten as “Although the efficient nucleation of HIO₃ and HIO₂ is overall consistent with the CLOUD measurements, this mechanism does not account for all HIO₃-induced nucleation in the real atmosphere.” in Lines 34-36 of the revised manuscript.

Comment 8: Line 48: might be rewritten as: the importance of the HIO₃-HIO₂-MSA nucleating mechanism may differ under distinct ambient conditions.

Response: According to this helpful suggestion, the sentence has been rewritten as “the importance of the HIO₃-HIO₂-MSA nucleation mechanism may differ under distinct ambient conditions” in Lines 47-48 of the revised manuscript.

Comment 9: Line 72: remove ‘and’

Response: According to the reviewer’s suggestion, the “and” has been removed in the Line 71 of revised manuscript.

Comment 10: Line 116: present -> presented

Response: The “present” has been corrected as “presented” in the Line 122 of revised manuscript.

Comment 11: Line 144: observed -> shown

Response: The “observed” has been corrected as “shown” in the Line 153 of revised manuscript.

Comment 12: Line 160: across-> through

Response: The “across” has been corrected as “through” in the Line 162 of revised manuscript.

Comment 13: Line 169: contribute to 74% of cluster formation

Response: Accordingly, the sentence has been corrected as “contribute to 74% of cluster formation” in the Line 171 of revised manuscript.

Comment 14: Line 214: access-> assess

Response: Thanks for the reviewer’s careful reading, the “access” has been corrected as “assess” in the Line 240 of revised manuscript.

Reference:

- [1] X.-C. He, Y.J. Tham, L. Dada, M. Wang, H. Finkenzeller, D. Stolzenburg, S. Iyer, M. Simon, A.K. Kürten, J. Shen, B. Roerup, M. Rissanen, S. Schobesberger, R. Baalbaki, D.S. Wang, T.K. Koenig, T. Jokinen, N. Sarnela, L.J. Beck, J. Almeida, S. Amanatidis, A. Amorim, F. Ataei, A. Baccarini, B. Bertozzi, F. Bianchi, S. Brilke, L. Caudillo, D. Chen, R. Chiu, B. Chu, A. Dias, A. Ding, J. Dommen, J. Duplissy, I.E. Haddad, L.G. Carracedo, M. Granzin, A. Hansel, M. Heinritzi, V. Hofbauer, H. Junninen, J. Kangasluoma, D. Kemppainen, C. Kim, W. Kong, J.E. Krechmer, A. Kvashin, T. Laitinen, H. Lamkaddam, C.P. Lee, K. Lehtipalo, M. Leiminger, Z. Li, V. Makhmutov, H.E. Manninen, G. Marie, R. Marten, S. Mathot, R.L. Mauldin, B. Mentler, O. Moehler, T. Mueller, W. Nie, A. Onnela, T. Petaja, J. Pfeifer, M. Philippov, A. Ranjithkumar, A. Saiz-Lopez, I. Salma, W. Scholz, S. Schuchmann, B. Schulze, G. Steiner, Y. Stozhkov, C. Tauber, A. Tome, R.C. Thakur, O. Vaisanen, M. Vazquez-Pufleau, A.C. Wagner, Y. Wang, S.K. Weber, P.M. Winkler, Y. Wu, M. Xiao, C. Yan, Q. Ye, A. Ylisirniö, M. Zauner-Wieczorek, Q. Zha, P. Zhou, R.C. Flagan, J. Curtius, U. Baltensperger, M. Kulmala, V.-M. Kerminen, T. Kurten, N.M. Donahue, R. Volkamer, J. Kirkby, D.R. Worsnop, M. Sipila, Role of iodine oxoacids in atmospheric aerosol nucleation, *Science* 371 (2021) 589–595.
- [2] H. Yu, L. Ren, X. Huang, M. Xie, J. He, H. Xiao, Iodine speciation and size distribution in ambient aerosols at a coastal new particle formation hotspot in China, *Atmos. Chem. Phys.* 19 (2019) 4025–4039.
- [3] J. Almeida, S. Schobesberger, A. Kürten, I.K. Ortega, O. Kupiainen-Määttä, A.P. Praplan, A. Adamov, A. Amorim, F. Bianchi, M. Breitenlechner, A. David, J. Dommen, N.M. Donahue, A. Downard, E. Dunne, J. Duplissy, S. Ehrhart, R.C. Flagan, A. Franchin, R. Guida, J. Hakala, A. Hansel, M. Heinritzi, H. Henschel, T. Jokinen, H. Junninen, M. Kajos, J. Kangasluoma, H. Keskinen, A. Kupc, T. Kurten, A.N. Kvashin, A. Laaksonen, K. Lehtipalo, M. Leiminger, J. Leppä, V. Loukonen, V. Makhmutov, S. Mathot, M.J. McGrath, T. Nieminen, T. Olenius, A. Onnela, T. Petäjä, F. Riccobono, I. Riipinen, M. Rissanen, L. Rondo, T. Ruuskanen, F.D. Santos, N. Sarnela, S. Schallhart, R. Schnitzhofer, J.H. Seinfeld, M. Simon, M. Sipilä, Y. Stozhkov, F. Stratmann, A. Tomé, J. Tröstl, G. Tsagkogeorgas, P. Vaattovaara, Y. Viisanen, A. Virtanen, A. Vrtala, P.E. Wagner, E. Weingartner, H. Wex, C. Williamson, D. Wimmer, P. Ye, T. Yli-Juuti, K.S. Carslaw, M. Kulmala, J. Curtius, U. Baltensperger, D.R. Worsnop, H. Vehkamäki, J. Kirkby, Molecular understanding of sulphuric acid-amine particle nucleation in the atmosphere, *Nature* 502 (2013) 359–363.
- [4] O. Kupiainen, I.K. Ortega, T. Kurtén, H. Vehkamäki, Amine substitution into sulfuric acid – ammonia clusters, *Atmos. Chem. Phys.* 12 (2012) 3591–3599.
- [5] K.D. Froyd, E.R. Lovejoy, Bond energies and structures of ammonia-sulfuric acid positive cluster ions, *J. Phys. Chem. A* 116 (2012) 5886–5899.
- [6] M. Sipilä, N. Sarnela, T. Jokinen, H. Henschel, H. Junninen, J. Kontkanen, S. Richters, J. Kangasluoma, A. Franchin, O. peräkylä, M.P. Rissanen, M. Ehn, H. Vehkamäki, T. Kurten, T. Berndt, T. Petäjä, D. Worsnop, D. Ceburnis, V.M. Kerminen, M. Kulmala, C. O'Dowd, Molecular-scale evidence of aerosol particle formation via sequential addition of HIO₃, *Nature* 537 (2016) 532–534.
- [7] C.D. O'Dowd, K. Hämeri, J. Mäkelä, M. Väkeva, P. Aalto, G. de Leeuw, G.J. Kunz, E. Becker, H.C. Hansson, A.G. Allen, R.M. Harrison, H. Berresheim, C. Kleefeld, M. Geever, S.G. Jennings, M. Kulmala, Coastal new particle formation: Environmental conditions and aerosol physicochemical characteristics during nucleation bursts, *J. Geophys. Res.-Atmos.* 107 (2002).
- [8] X.-C. He, S. Iyer, M. Sipilä, A. Ylisirniö, M. Peltola, J. Kontkanen, R. Baalbaki, M. Simon, A. Kürten, Y.J. Tham, J. Pesonen, L.R. Ahonen, S. Amanatidis, A. Amorim, A. Baccarini, L. Beck, F. Bianchi, S. Brilke, D. Chen, R. Chiu, J. Curtius, L. Dada, A. Dias, J. Dommen, N.M. Donahue, J. Duplissy, I. El

Haddad, H. Finkenzeller, L. Fischer, M. Heinritzi, V. Hofbauer, J. Kangasluoma, C. Kim, T.K. Koenig, J. Kubečka, A. Kvashnin, H. Lamkaddam, C.P. Lee, M. Leiminger, Z. Li, V. Makhmutov, M. Xiao, R. Marten, W. Nie, A. Onnela, E. Partoll, T. Petäjä, V.-T. Salo, S. Schuchmann, G. Steiner, D. Stolzenburg, Y. Stozhkov, C. Tauber, A. Tomé, O. Väisänen, M. Vazquez-Pufleau, R. Volkamer, A.C. Wagner, M. Wang, Y. Wang, D. Wimmer, P.M. Winkler, D.R. Worsnop, Y. Wu, C. Yan, Q. Ye, K. Lehtinen, T. Nieminen, H.E. Manninen, M. Rissanen, S. Schobesberger, K. Lehtipalo, U. Baltensperger, A. Hansel, V.-M. Kerminen, R.C. Flagan, J. Kirkby, T. Kurtén, M. Kulmala, Determination of the collision rate coefficient between charged iodine acid clusters and iodine acid using the appearance time method, *Aerosol Sci. Tech.* 55 (2021) 231-242.

[9] L. Liu, S. Li, H. Zu, X. Zhang, Unexpectedly significant stabilizing mechanism of iodous acid on iodine acid nucleation under different atmospheric conditions, *Sci. Total Environ.* 859 (2023) 159832.

[10] S. Zhang, S. Li, A. Ning, L. Liu, X. Zhang, Iodous acid - a more efficient nucleation precursor than iodine acid, *Phys. Chem. Chem. Phys.* 24 (2022) 13651–13660.

[11] R. Zhang, H.B. Xie, F. Ma, J. Chen, S. Iyer, M. Simon, M. Heinritzi, J. Shen, Y.J. Tham, T. Kurtén, D.R. Worsnop, J. Kirkby, J. Curtius, M. Sipilä, M. Kulmala, X.C. He, Critical Role of Iodous Acid in Neutral Iodine Oxoacid Nucleation, *Environ. Sci. Technol.* 56 (2022) 14166–14177.

[12] K.-M. Oona, O. Tinja, Atmospheric Cluster Dynamics Code Technical manual, https://github.com/tolenius/ACDC/blob/main/ACDC_Manual_2020_11_25.pdf (2020).

[13] L.J. Beck, N. Sarnela, H. Junninen, C.J.M. Hoppe, O. Garmash, F. Bianchi, M. Riva, C. Rose, O. Peräkylä, D. Wimmer, O. Kausiala, T. Jokinen, L. Ahonen, J. Mikkilä, J. Hakala, X.C. He, J. Kontkanen, K.K.E. Wolf, D. Cappelletti, M. Mazzola, R. Traversi, C. Petroselli, A.P. Viola, V. Vitale, R. Lange, A. Massling, J.K. Nøjgaard, R. Krejci, L. Karlsson, P. Zieger, S. Jang, K. Lee, V. Vakkari, J. Lampilahti, R.C. Thakur, K. Leino, J. Kangasluoma, E.M. Duplissy, E. Siivola, M. Marbouti, Y.J. Tham, A. Saiz-Lopez, T. Petäjä, M. Ehn, D.R. Worsnop, H. Skov, M. Kulmala, V.M. Kerminen, M. Sipilä, Differing Mechanisms of New Particle Formation at Two Arctic Sites, *Geophys. Res. Lett.* 48 (2021).

[14] NASA POWER. Data access viewer. <https://power.larc.nasa.gov/data-accessviewer/>, (2022).

[15] L.L.J. Quéléver, L. Dada, E. Asmi, J. Lampilahti, T. Chan, J.E. Ferrara, G.E. Copes, G. Pérez-Fogwill, L. Barreira, M. Aurela, D.R. Worsnop, T. Jokinen, M. Sipilä, Investigation of new particle formation mechanisms and aerosol processes at Marambio Station, Antarctic Peninsula, *Atmos. Chem. Phys.* 22 (2022) 8417–8437.

[16] H. Berresheim, T. Elste, K. Rosman, M. Dal Maso, H.G. Tremmel, J.M. Mäkelä, A.G. Allen, M. Kulmala, H.-C. Hansson, Gas-aerosol relationships of H₂SO₄, MSA, and OH: Observations in the coastal marine boundary layer at Mace Head, Ireland, *J. Geophys. Res.-Atmos.* 107 (2002) PAR 5-1–PAR 5-12.

[17] R. Salignat, M. Rissanen, S. Iyer, J.-L. Baray, P. Tulet, J.-M. Metzger, J. Brioude, K. Sellegri, C. Rose, Measurement Report: Insights into the chemical composition of molecular clusters present in the free troposphere over the Southern Indian Ocean: observations from the Maïdo observatory (2150 m a.s.l., Reunion Island), *EGU sphere* (2023) 1–41.

[18] M. Kulmala, T. Petäjä, T. Nieminen, M. Sipilä, H.E. Manninen, K. Lehtipalo, M. Dal Maso, P.P. Aalto, H. Junninen, P. Paasonen, I. Riipinen, K.E.J. Lehtinen, A. Laaksonen, V.-M. Kerminen, Measurement of the nucleation of atmospheric aerosol particles, *Nature Protocols* 7 (2012) 1651-1667.

[19] D. Xia, J. Chen, H. Yu, H.B. Xie, Y. Wang, Z. Wang, T. Xu, D.T. Allen, Formation Mechanisms of Iodine-Ammonia Clusters in Polluted Coastal Areas Unveiled by Thermodynamics and Kinetic Simulations, *Environ. Sci. Technol.* 54 (2020) 9235-9242.

[20] M.J. McGrath, T. Olenius, I.K. Ortega, V. Loukonen, P. Paasonen, T. Kurtén, M. Kulmala, H.

Vehkamäki, Atmospheric Cluster Dynamics Code: a flexible method for solution of the birth-death equations, *Atmos. Chem. Phys.* 12 (2012) 2345–2355.